Key Landscapes for Conservation Land Cover and Change Monitoring, Thematic and Validation Datasets for Sub-Saharan Africa

Zoltan Szantoi[1,2], Andreas Brink[1], Andrea Lupi[1], Claudio Mammone[3], Gabriel Jaffrain[4]

[1]European Commission, Joint Research Centre, 21027 Ispra, Italy
[2]Department of Geography and Environmental Studies, Stellenbosch University, Stellenbosch 7602, South Africa
[3]e-Geos - an ASI / Telespazio Company, Contrada Terlecchie, 75100, Matera, Italy
[4]IGN FI - Ingénierie Géographique Numérique Française à l'International, 75012 Paris, France

Correspondence to: Zoltan Szantoi (zoltan.szantoi@ec.europa.eu)

Abstract. Mounting social and economic demands on natural resources increasingly threaten key areas for conservation in Africa. Threats to biodiversity pose an enormous challenge to these vulnerable areas. Effective protection of sites with strategic conservation importance requires timely and highly detailed geospatial monitoring. Larger ecological zones and wildlife corridors warrant monitoring as well, as these areas have an even higher degree of pressure and habitat loss. To address this, a satellite imagery based monitoring workflow to cover at-risk areas at various details was developed. During the program's first phase, a total of 560442km^2 area in Sub-Saharan Africa was covered, from which 153665km^2 were mapped with 8 land cover classes while 406776km^2 were mapped with up to 32 classes. Satellite imagery was used to generate dense time series data from which thematic land cover maps were derived. Each map and change map were fully verified and validated by an independent team to achieve our strict data quality requirements. The independent validation datasets for each KLCs are also described and presented here (The dataset available at Szantoi et al., 2020A https://doi.pangaea.de/10.1594/PANGAEA.914261).

1 Introduction

Key Landscapes for Conservation (MacKinnon et al., 2015) (KLC) are defined as areas vast enough to sustain large wild animals (e.g. Big Five game) within functioning biomes that face pressure from various external factors such as poaching, agriculture expansion and urbanization. Land use changes cause loss in both flora and fauna by altering wild animal movements that can lead to decreases in population size over time (Di Minin et al., 2016; van der Meer, 2018). The livelihood of People and wildlife in Africa that depend on natural resources face increasing pressure from resource consumption by the continent's growing population, set to reach 2 billion by 2040 (MacKinnon et al., 2015, Di Minin et al., 2016). The representative location

types, often transboundary, of the KLCs uniquely positions them as benchmarks for their natural resources management to generate steady income for the local residents while protecting their wildlife (MacKinnon et al., 2015). Benchmarking activities of this kind require highly accurate thematic land cover/change (LCC) map products. Although LCC maps exist for many areas within Africa, the majority of products only cover protected areas with some buffer zones (Szantoi et al., 2016). However, continental and global mapping efforts reported thematic accuracies for such land cover maps between 67%-81%, with lower class accuracies reported in many cases (Mora et al., 2014). Differences in legends and unstandardized methods make these cases difficult to use for monitoring, modelling or change detection studies. In order to use various LC and LCC products together (i.e. modelling, policy making), land cover class definitions should be standardized to avoid discrepancies in thematic class understanding. Not all users (international organizations, national governments, civil societies, researchers) have the capabilities to readjust such maps (Saah et al., 2020). To accommodate diverse user profiles, a common processing scheme is employed. The resulting datasets can be utilized through various platforms and systems.

This work adopts the Land Cover Classification Scheme of the Food and Agriculture Organization (FAO LCCS, DiGregorio 2005), an internationally approved ISO standard approach. The presented datasets in this paper are produced within the Copernicus High Resolution Hot Spot Monitoring (C-HSM) activity of the Copernicus Global Land Service. All C-HSM products feature the same thematic land cover legend and geometric accuracy, and were processed and validated following the same methodology. All products, including the C-HSM data, are free and open to any user with guaranteed long-term maintenance and availability under the Copernicus license.

Copernicus serves as an operational program where data production takes place on a continuous basis. This paper presents twelve KLC land cover [change] datasets that cover up to 560442km^2 terrestrial land area in Sub-Saharan Africa (SSA) mapped under the first phase (Phase 1) of the C-HSM activity. The datasets are based on freely available medium spatial resolution data. Each of the KLCs were individually validated for both present (~2016) and change (~2000) dates. The developed processing chain always consists of preliminary data assessment for availability, pre and post processing as well as fully independent quality verification and validation steps. For the latter, a second dataset called validation data is presented.

Several recent studies call for the sharing of product validation datasets (Fritz et al., 2017; Tsendbazar et al., 2018), especially if a collection received financial support from government grants (Szantoi et al., 2020B). Accordingly, the validation datasets (LC/LCC) associated with each of the KLCs are also shared.

2 Study Area

The provided thematic datasets concentrate on Sub-Saharan Africa. This region is on the frontline of natural and human induced changes. The selection of areas were conducted based on present and future pressures envisioned and predicted (MacKinnon et al., 2015). In this first phase (Phase 1), 12 large areas totalling 560442km^2 in SSA were selected, mapped and validated (Figure 1). These areas cover various ecosystems and generally reside in transboundary regions (Table 1, Figure 1).

Table 1 Mapped Key Landscapes for Conservation (KLC) within Phase 1. Mapping detail refers to the employed classification scheme – Dichotomous (D) and Modular (M); see it in the Data collection and mapping guidelines section.

KLC (MacKinnon et al., 2015)	**Code**	**Mapping detail**	**Ecoregion** (Dinerstein et al., 2017)	**Country**	**Area (km^2)**
Takamanda	CAF01	M	Cameroon Highlands forests, Cross-Sanaga-Bioko coastal forests, Guinean and Northern Congolian Forest-Savanna	Nigeria, Cameroon	79534
Greater Virunga	CAF02	M	Albertine Rift montane forests Victoria Basin forest-savanna	DRC, Uganda, Rwanda	39062
Manovo-Gounda-St Floris-Bamingui	CAF06	M	East Sudanian savanna	Central African Republic, Chad	96965
Salonga	CAF07	D	Central Congolian lowland forests	DRC	66625
Upemba	CAF11	M	Central Zambezian wet miombo woodlands	DRC	47318
Lomami	CAF15	M	Central Congolian lowland forests	DRC	30924
Mbam Djerem	CAF16	D	Northern Congolian Forest-Savanna Northwest Congolian lowland forests	Cameroon	11510
Yangambi*	CAF99	M	Northeast Congolian lowland forests	DRC	7276
Great Limpopo	SAF02	M	Zambezian mopane woodlands Limpopo lowveld	Mozambique, South Africa, Zimbabwe	65475
North and South Luangwa	SAF14/ SAF15	D	Dry miombo woodlands Central Zambezian wet miombo woodlands	Zambia	34880
Comoe-Mole	WAF05	D	West Sudanian savanna Guinean forest-savanna	Ivory Coast, Ghana	40648
Tai-Sapo	WAF10	M	Western Guinean lowland forests	Ivory Coast, Liberia	40219
Area total					**560442**

* - it is not included in MacKinnon et al. (2015) list. DRC - Democratic Republic of the Congo

Figure 1 Spatial distribution of the Key Landscapes for Conservation Phase 1 areas.

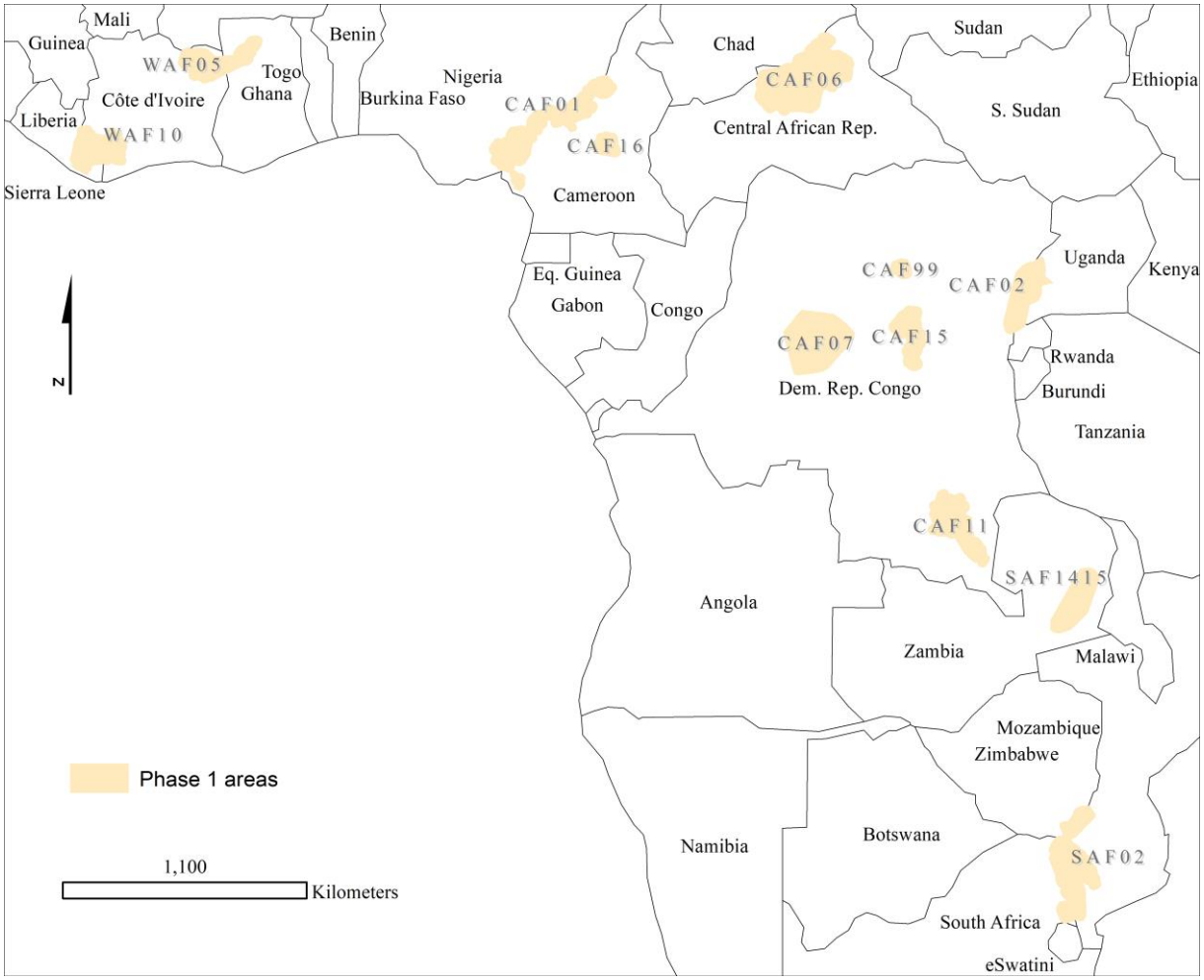

3 Data and Method

3.1 Thematic dataset production

The production workflow for the entire process is shown in Figure 2. Each stage is explained in details in the below sections.

Figure 2. Overall production workflow

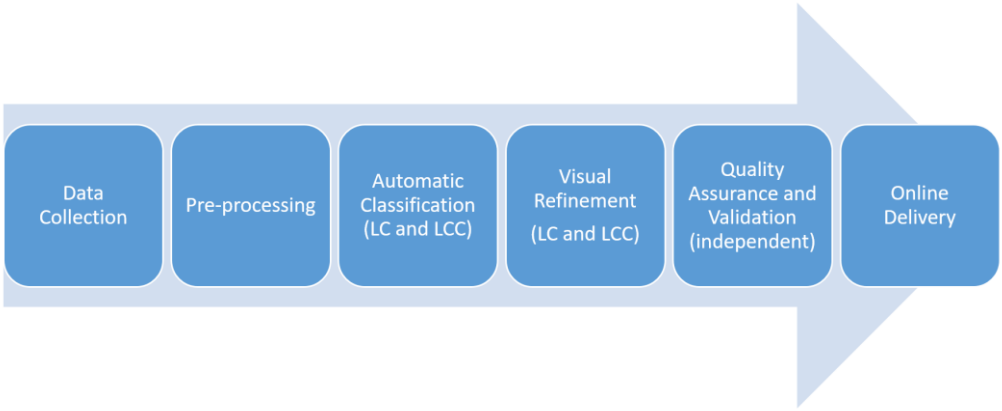

3.1.1 Data collection and mapping guidelines

Landsat TM, ETM+ and OLI imagery at Level1TP processing level were used in the production of the Phase 1 land cover and change maps. The Level1TP data was further corrected for atmospheric conditions to produce surface reflectance products for the classification phase. The atmospheric correction module was implemented based on the 6S as a direct radiative transfer model (Masek et al., 2006). The Shuttle Radar Topography Mission (30m or 90m) Digital Elevation Model was used to estimate the target height and slope, as well as correct the surface sun incidence angles to perform an optional topographic correction. The Aerosol Optical Thickness (AOT) was estimated directly from either Landsat or Sentinel-2 data (Hagolle et al., 2015). Based on the area's meteo-climatic conditions (climate profile and precipitation patterns), season specific satellite image data were selected for each KLC (Table 1). Due to data scarcity for many areas, especially for the change maps (year 2000), imagery was collected for a target year ± 3 years. In extreme cases, (±) 5 years were allowed, or until four cloud free observations per pixel for the specified date were reached. The cloud and shadow masking procedure was based on the FMASK algorithm (Zhu et al., 2015).

3.1.2 Land cover classification system

All thematic maps were produced either at *Dichotomous* or at both Dichotomous and *Modular* levels within the Land Cover Classification System (LCCS) developed by the Food and Agriculture Organization of the United Nations and the United Nations Environment Programme (Di Gregorio, 2005). The LCCS (ISO 19144-2) is a comprehensive hierarchical classification system that enables comparison of land cover classes regardless of geographic location or mapping date and scale (Di Gregorio, 2005). At the *Dichotomous* level, the system distinguishes eight major LC classes. At the *Modular* level, thirty-two LC classes were used (Table 2).

Table 2 Dichotomous and Modular thematic land cover/use classes.

Dichotomous level	Mapcode	Modular level	Mapcode
Cultivated and Managed Terrestrial Area (A11)	3	continuous large to medium sized field (>2 ha) of tree crop cover: plantation	31
		continuous small sized field (<2 ha) of tree crop cover: plantation	32
		continuous large to medium sized field (>2 ha) of tree crop cover: orchard	33
		continuous small sized field (<2 ha) of tree crop cover: orchard	34
		continuous large to medium sized field (>2 ha) of shrub crop	55
		continuous small sized field (<2 ha) of shrub crop	56
		continuous large to medium sized field (>2 ha) of herbaceous crop	59
		continuous small sized field (<2 ha) of herbaceous crop	60
Natural and Semi-Natural Primarily Terrestrial Vegetation (A12)	4	continuous closed (>70-60) trees	77
		continuous open general (70-60)-(20-10)% trees	78
		continuous closed to open (100-40)% shrubs	112
		continuous open (40 - (20-10)%) shrubs	116
		continuous closed to open (100-40)% herbaceous vegetation	148
		continuous open (40 - (20-10)%) herbaceous vegetation	152
Cultivated Aquatic or Regularly Flooded Area (A23)	6	continuous large to medium sized field (>2 ha) of woody crops	155
		continuous small sized field (<2 ha) of woody crops	156
		continuous large to medium sized field (>2 ha) of graminoid crops	159
		continuous small sized field (<2 ha) of graminoid crops	160
Natural And Semi-Natural Aquatic or Regularly Flooded Vegetation (A24)	7	closed (>70-60)% trees	165
		open general (70-60)-(20-10)% trees	166
		closed to open (100-40)% shrubs	171
		very open (40 - (20-10)%) shrubs	175
		closed to open (100-40)% herbaceous vegetation	178
		very open (40 - (20-10)%) herbaceous vegetation	182
Artificial Surfaces and Associated Area (B15)	10	built up area	184
		non built up area	185
Bare Area (B16)	11	Bare area	11
Artificial Waterbodies, Snow and Ice (B27)	13	artificial waterbodies (flowing)	186
		artificial waterbodies (standing)	187
Natural Waterbodies, Snow and Ice (B28)	14	natural waterbodies (flowing)	190
		natural waterbodies (standing)	191
		snow	192

		ice	193

3.1.3 Automatic classification

Based on the pre-selected imagery data, Dense Multitemporal Timeseries (DMT) based vegetation indices were generated to reduce data dimensionality and enhance the signal of the surface target. The DMT for each KLCs were based on the pre-processed and geometrically coregistered data, forming a geospatial datacube (Strobl et al., 2017). In addition, three vegetation indices were calculated to aid the separation of terrestrial vs. aquatic (NDFI), vegetated vs. barren (SAVI), and evergreen vs. deciduous vegetation areas (NBR).

The indices are (per Landsat spectral bands):

Normalized Difference Flooding Index (NDFI) $$NDFI = \frac{(RED - SWIR2)}{(RED + SWIR2)} \quad (1)$$

Soil Adjusted Vegetation Index (SAVI) $$SAVI = \frac{1.5 \times (NIR - RED)}{(NIR + RED + 0.5)} \quad (2)$$

Normalized Burn Ratio (NBR) $$NBR = \frac{(NIR - SWIR2)}{(NIR + SWIR2)} \quad (3)$$

All the pre-processed data (spectral bands and the DMT based indices) were fed into the Support Vector Machine supervised classification model. The Support Vector Machine classifier can handle data with high dimensionality and performs well with mapping heterogeneous areas, including vegetation community types (Szantoi et al., 2013). To produce the thematic maps, the Minimum Mapping Unit concept used by Szantoi et al. (2016) was employed. Individual pixels (with corresponding land cover class information) were assigned into objects, where the minimum size of an object was set at 0.5-5 hectares, as a compromise between technical feasibility (pixel size) and the general size of the observable features (various land cover classes). Still, classification errors (omission and commission of various classes) and false alarms (for land cover change) arose due to the data availability (cloud cover, no data) and the seasonal behaviour of the land cover (e.g. rapid foliage change). To correct these errors, expert human image interpretation skills and knowledge that improved the outputs from the automated process were employed.

3.1.4 Land cover change detection

Land cover change was interpreted as a categorical change in which a particular land cover was replaced by another land cover. As an example of conversion, the change of Cultivated and Managed Terrestrial Areas (A11) into a Natural and Semi-Natural Terrestrial Vegetation (A12) or a Cultivated and Managed Terrestrial Areas (A11) into Artificial Surfaces and Associated Areas (B15) can be mentioned. The basic condition for LC changes identification was the detection of changes in spectral reflectance within specific image bands of the employed satellite imagery, but such changes were further evidenced by other interpretation parameters such as shape and texture patterns. In regards to our methodology, images acquired in two or more different timeframes were used in the identification process. Furthermore, land cover changes were characterised by those changes that have longer than yearly and/or seasonal periodicity (dry/wet season). Urban sprawl, tree plantations (large or

small) to replace herbaceous crops (large or small), tree covers (closed or open) or the creation of a new water reservoir undergo long-term changes that classify as actual LCCs. In our workflow, the LCC process followed the same image pre-processing steps as the LC method, and an independent classification (similarly to the LC procedure) of the past date was performed. Finally, the LC and the LCC products were compared and change polygons were extracted. As with the LC product, the visual refinement was an important step to produce accurate LCC polygons.

3.2 Validation dataset production

The validation datasets (Table 3, Figure 3) were individually created for each KLCs. The validation datasets (points) were generated using a stratified random sampling procedure. This assured a sufficient estimation for all land cover and land cover change classes according to their frequency of occurrence. The following formula (Gallaun et al., 2015) was used to determine the minimum number of validation points (per class per KLC):

$$n_c = \frac{p_c(1-p_c)}{\sigma_c^2}, c = 1, \dots, L \quad (4)$$

n_c number of sampling units for class c

p_c estimated error rate for class c

σ_c accepted standard error of the error of commission for class c

L number of classes

In cases where classes covered smaller areas in total, additional sampling units were allocated according to the Neyman optimal allocation in order to minimize the variance of the estimator of the overall accuracy for the total sample size [n] (Gallaun et al., 2015; Stehman, 2012):

$$n_c = \frac{nN_c\sigma_c}{\sum_{k=1}^{L} N_k\sigma_k} \quad (5)$$

n_c sample size for class c

N_c population size for class c

σ_c estimated error rate for class c

L number of classes

N_k population size for class k

σ_k estimated error rate for class k

At least two independent data analysts (blind and plausibility interpretation process) evaluated all accuracy points. Some points were excluded from the accuracy statistics due to an error/disagreement during the evaluation procedure (Table 3 - "Number of points LC/LCC"). The *blind* process attempt to interpret all validation points was based on available ancillary data (i.e. higher resolution imagery), without direct comparison to the generated LC/LCC maps. The *plausibility* process reviewed every point whose the blind interpretation did not match the corresponding LC/LCC value (disagreement between the LC/LCC data and the blind interpretation). After this review, the final validation reference is established.

Table 3 Validation dataset attributes

KLC Code	Mapping detail	Number of LC classes	Number of LCC classes	Number of points LC/LCC
CAF01	M	26	12	3849
CAF02	M	26	18	4465
CAF06	M	19	13	4151
CAF07	D	5	3	1364
CAF11	M	23	15	3785
CAF15	M	17	9	3687
CAF16	D	7	2	1254
CAF99	M	17	14	2727
SAF02	M	26	19	3367
SAF14/15	D	6	3	1335
WAF05	D	8	3	1264
WAF10	M	22	12	4423

Figure 3 Spatial distribution of the validation datasets within each Key Landscapes for Conservation areas.

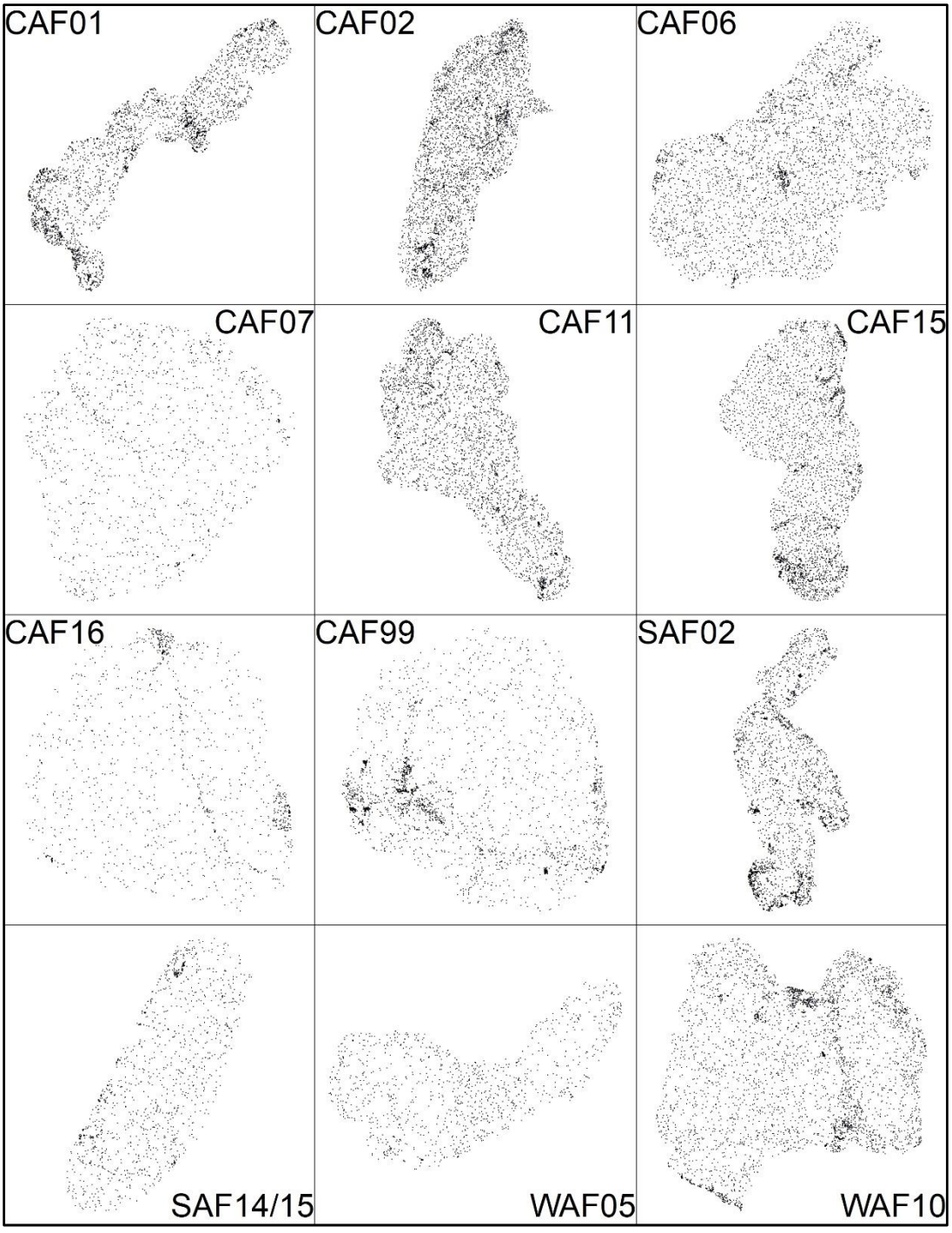

4. Assessment - Data Quality

Technical Validation

Spatial, temporal and logical consistency was assessed by an independent procedure from the producer to determine the products positional accuracy, the validity of data with respect to time (seasonality), and the logical consistency of the data (topology, attribution and logical relationships). A Qualitative-systematic accuracy assessment was also performed wall-to-wall through a systematic visual examination for a) global thematic assessment b) expected size of polygons (Minimum Mapping Unit (MMU)), c) seasonal effects and d) spatial patterns (i.e. following correct edges).

The quantitative accuracy assessment (i.e. validation) results are shown in Table 4 (overall accuracies), and in the Appendix (thematic class accuracies per KLC, Appendix A). Generally, the program aimed at a minimum of 85% overall accuracy for each product (KLC) and a minimum of 75% thematic accuracy (Producer's and User's) for each class within each KLC. The land cover change (LCC) accuracy should be >72%. In exceptional cases, the thematic accuracies might be lower than the threshold due to the difficulty to discriminate a particular class in a certain KLC. Figure 4 shows the final LC and LCC products classified at the dichotomous LCCS level while Figures 5A and 5B show the final LC and LCC products classified at the modular LCCS level.

Table 4 Achieved overall accuracies for land cover mapping in (%)

KLC Code	Land cover map [200X]*	Reference date	Land cover map [201X]*	Reference date
CAF01	94.31	2000	92.26	2016
CAF02	91.93	2001	90.09	2015
CAF06	87.82	2003	85.72	2015
CAF07	99.40	2000	99.60	2016
CAF11	96.10	2000	95.27	2016
CAF15	99.10	2000	99.10	2016
CAF16	99.10	2000	98.90	2016
CAF99	98.12	2000	98.51	2016
SAF02	93.32	2002	92.8	2016
SAF14/15	97.70	2000	97.70	2015
WAF05	97.10	2000	96.40	2015
WAF10	98.43	2001	98.78	2016

*[200X] and [201X] refer to the year the map represent; the exact year is in the "Reference date" columns

Figure 4 Key Landscapes for Conservation - Dichotomous classification level. The boundaries (black polygons) represent protected areas (IUCN category I-IV) within the KLCs. Both, land cover and land cover change, are presented for each KLC.

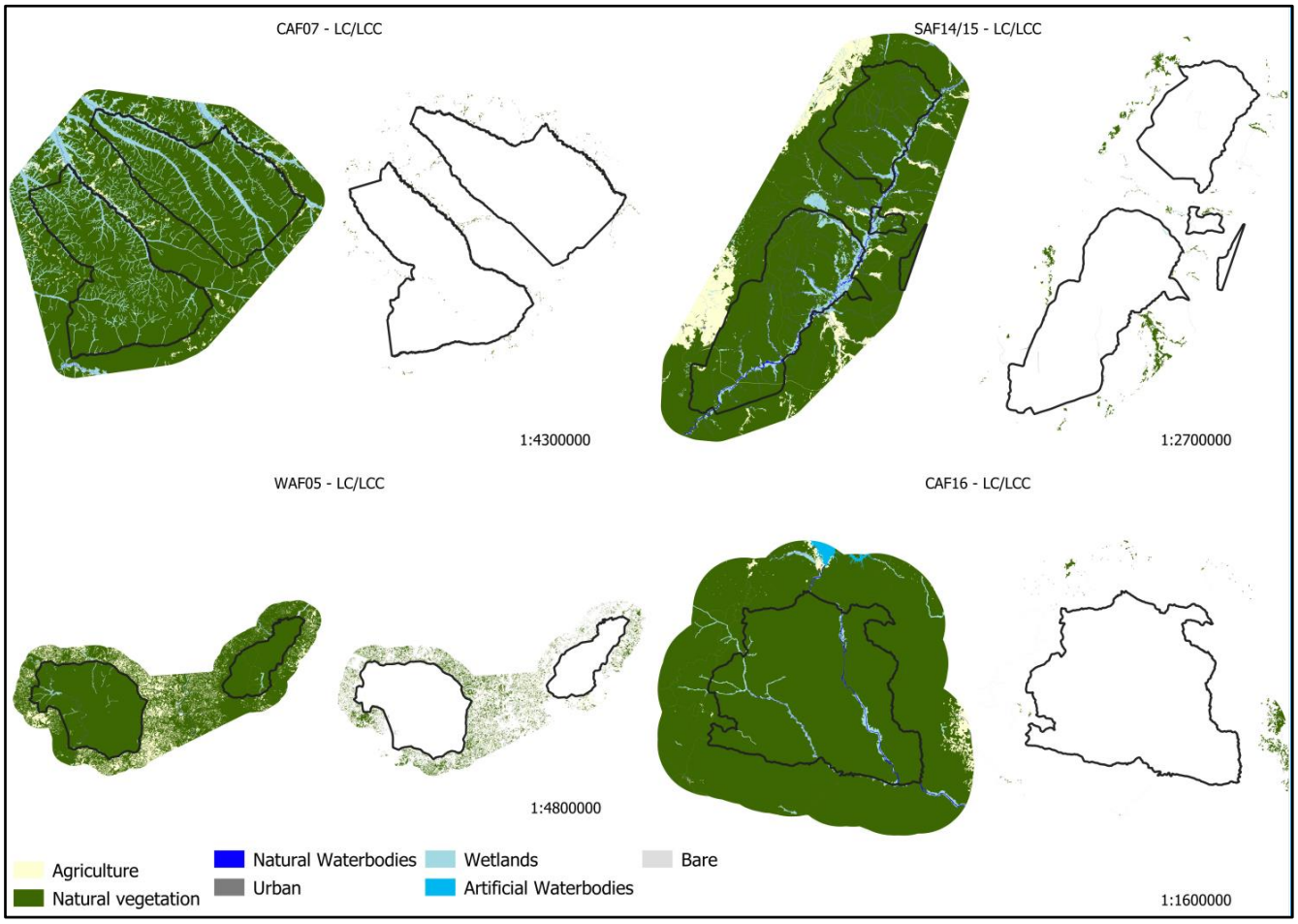

Figure 5A Key Landscapes for Conservation - Modular classification level. The boundaries (black polygons) represent protected areas (IUCN category I-IV) within the KLCs. Both, land cover and land cover change, are presented for each KLC.

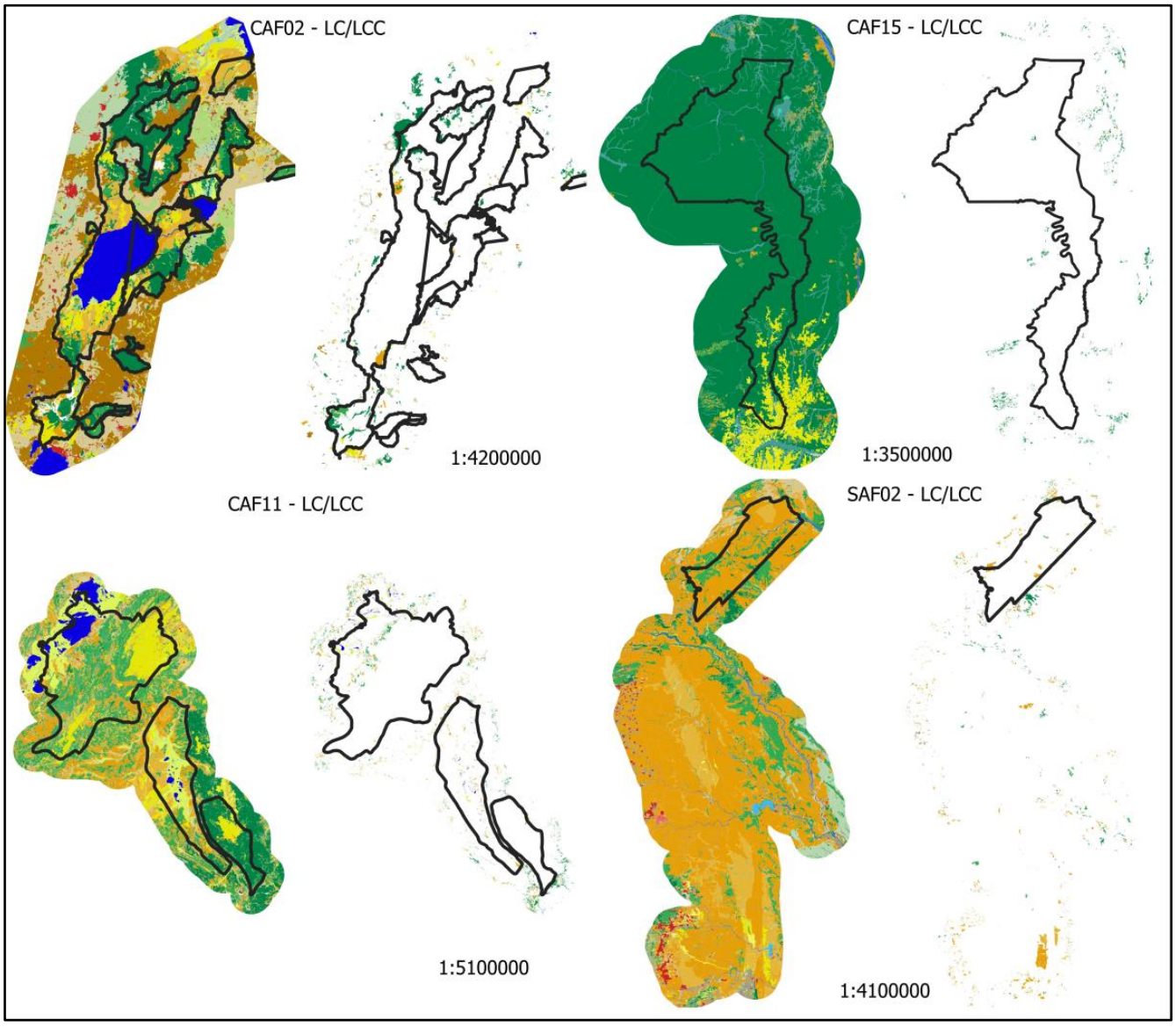

Figure 5B Key Landscapes for Conservation - Modular classification level. The boundaries (black polygons) represent protected areas (IUCN category I-IV) within the KLCs. Both land cover and land cover change are presented for each KLC.

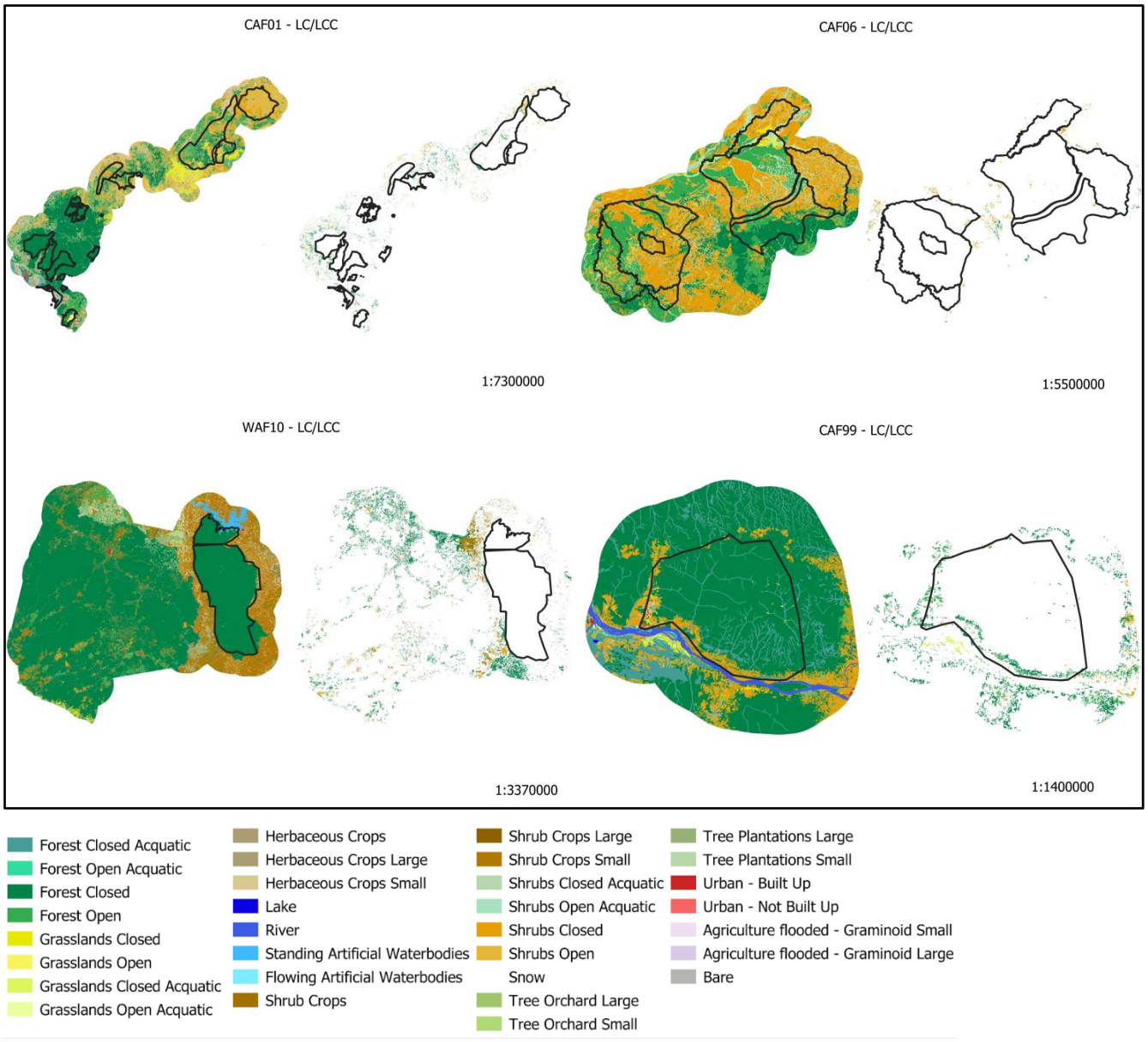

5. Discussion

There is a direct relationship between population growth, agricultural expansion, energy demand and pressure on land. With the current state of development, population increase and economic growth, a large portion of the Sub-Saharan population

depend on the remaining natural resources to meet their food and energy needs (Brink et al., 2012). The demands of social and economic growth require additional land, typically at the expense of previously untouched areas. Areas under protection (i.e. National Parks) that remain well-preserved (see Figures 4 and 5AB) often have regions in close proximity under tremendous pressure. Such areas (many times transboundary ones) need very accurate monitoring and base maps, which are provided through this work; especially as areas shared between and/or among countries are frequently not mapped with a common legend, if mapped at all. The presented KLC datasets can be used for continuous land cover/use monitoring, evaluation of management practices/effectiveness, endowment for scientific counsel, habitat modelling, information dissemination and capacity building in their corresponding countries and to manage natural resources such as forests, soil, biodiversity, ecosystem services and agriculture (Tolessa et al., 2017). Furthermore, regional climate change, biogeochemical and hydrologic models are currently capable of using high resolution LC data for predictions in general (Nissan et al., 2019) and spatially focused (i.e. Africa) (Sylla et al., 2016; Vondou and Haensler, 2017).

The validation datasets are independently collected and verified through a robust procedure. Validation datasets can then be used for additional land cover mapping, creating spectral libraries, and for the validation of other local, regional and global datasets. It is important that various land cover products can be used or compared against one another regardless of their geographic origins. Here, twelve land cover maps for different areas in Sub-Saharan Africa where quality land cover products are missing (Marshall et al., 2017) were introduced. These products come with land cover change information as well, generally dating back to year 2000 (±3 years). All data were produced using the unified Land Cover Classification System. The LCCS's modular level can be applied to local scales through its very detailed classes (here 32).

5.1 Drivers of change

Geist and Lambin (2002) describe the human driving forces of land-cover changes as an interlinking of three key variables: expansion of agriculture, extraction of wood, and development of infrastructure. The main land cover dynamic in Sub-Saharan Africa can be explained by the first two variables, where agriculture expansion is further subdivided into shifting cultivation, permanent cultivation, and cattle ranching, and wood extraction is subdivided into commercial wood extraction (clear-cutting, selective harvesting), fuelwood extraction, pole wood extraction and charcoal production. Although the driving force behind the clearing of natural vegetation has traditionally been predominantly attributed to the expansion of new agricultural land areas (including investments in large-scale commercial agriculture) (Brink and Eva, 2009), firewood extraction and charcoal production are also key factors in forest, woodland and shrub land degradation throughout the region. This land cover dynamic is not just a by-product of greater forces such as logging for timber and agricultural expansion, but stems from a specific need to satisfy energy demand (European Commission, 2018); in fact, in Sub-Saharan Africa, the main use of extracted wood is for energy production (Kebede et al., 2010). Although the region possesses a huge diversity of energy sources such as oil, gas, coal, uranium, and hydropower, the local infrastructure and use of these commercial energy sources are very limited. Traditional sources of energy in the form of firewood and charcoal account for over 75% of the total energy use in the region (Kebede et al., 2010). Efforts to meet the population and economic demands in sub-Saharan Africa while preserving

biodiversity and ecosystem functioning require informed decision-making. The global component of the Copernicus Land Service (Copernicus Global Land), in particular the High-Resolution Hot Spot Monitoring component, present a unique opportunity for such information gathering.

5.2 Sources of errors

As the applied LCCS allows very detailed hierarchical classification, some classes can be difficult to distinguish from each other. This is especially true in Africa's vast and very heterogeneous landscapes where agricultural land use is mainly smallholder based (i.e. very small plots), while shifting cultivation is mostly due to the lack of fertilizers and weak soil, leading to land abandonment. Landscapes are generally not composed of clearly fragmented and well identifiable cover formation. In this region, landscapes usually form a continuum of various cover (vegetation) formations that might include different layers of tree, shrub and herbaceous. These variations combined with differences in vegetation density (open vs. closed) and heights makes class assignments challenging. Moreover, some specific agriculture classes distinguish even the cultivation type, e.g. differentiating between fruit tree plantations from tree plantations for timber. Thus, the discrimination of such classes is very difficult and might introduce classification errors.

Apart from the land cover classification, errors could also be introduced due to climate-induced variability, such as leaf phenology where deciduous vegetation might appear bare during a dry period (season).

At a more general level, difficulties in identifying between aquatic or regularly flooded surfaces and terrestrial areas have been observed in certain KLCs, especially when flooded periods are short.

5.3 Datasets current and future use

The C-HSM datasets have been widely used by policy makers (African and European partners) to help identify areas prone to change due to human activities. For example, COFED (Support Unit for the [DRC] National Authorizing Officer of the European Development Fund) the EEAS (European External Action Service) of the DRC manage an envelope of EUR120m, allocated for five protected areas in the DRC (Virunga, Garamba, Salonga, Upemba and the Yangambi biosphere), where they use the C-HSM products for planning and for investment strategies (i.e. hydropower). Another example comes from West Africa, where NGOs (e.g. Wild Chimpanzee Foundation), public-benefit enterprises (i.e. German Society for International Cooperation - GIZ) as well as national authorities (i.e. l'Office Ivoirien des Parcs et Réserves - OIPR) use the data to identify areas under pressure for agriculture (cocoa, oil palm, rubber, coconut) and human-wildlife conflicts in Cote d'Ivoire, Ghana and Liberia.

6. Data Availability

The data are provided in a shapefile (*.shp) format, polygon geometry for the land cover and change datasets and point geometry for the validation datasets. The presented data is in the World Geodetic System 1984 Geographic Coordinate System

(GCS) (EPSG:4326) and its datum (EPSG:6326). The validation data, beside using the same GCS, also have the Africa Albers Equal Area Conic (EPSG:102022) projected coordinate system.

Each of the 12 KLCs is described by two vector layers: a Land Cover (LC) layer and a Land Cover Change (LCC) layer. The LC layer is a wall-to-wall map, covering the entire Area of Interest (AOI). The LC temporal reference for the project is the year 2016, although for each area the actual "mapping year" is noted in the file name (i.e. CAF01_2016) and generally refers to the year in which the largest number of satellite images were used for the classification. The LCC layer provides a partial coverage of the AOI, as it contains only the areas (polygons) where thematic change occurred compared to the LC layer. The LCC temporal reference is the year 2000 (+/- 3 years), noted in the file name (i.e. CAF01_2000).

Each LC and LCC shapefiles comes with its corresponding attribute table, where two or three attributes are present: [mapcode_A] - dichotomous class, [mapcode_B] - modular class, [name_A] - corresponding dichotomous classnames (KLCs classified only at the dichotomous level, [name_B] - corresponding modular classname.

Validation points dataset:

Each of the 12 areas has been quantitatively validated using a spatially specific point dataset. These datasets were generated through the method described in point 3.2, and each point was used to verify the correctness of the LC/LCC maps. The corresponding data in the attribute table are: LC - [plaus201X] and LCC - [plaus200X]. Both [plaus201X] and [plaus200X] attributes refer to the most detailed classification level attributes [mapcode_A or mapcode_B] present in the LC and LCC datasets (shapefiles). The plaus201X and plaus200X refer to the year the validation sets represent, as these can be different among KLCs; the exact year is always noted in the columns' names (e.g. plaus2000, plaus2016).

The naming of all attributes follow the same structure in all data. Please see the details in the Appendix Information and Supplementary Information section.

The complete package (all datasets) is available for download at https://doi.pangaea.de/10.1594/PANGAEA.914261, or individually as source datasets.

Besides archiving the datasets at PANGEA (www.pangea.eu) with corresponding Digital Object Identifiers, the Copernicus Hot-Spot website (https://land.copernicus.eu/global/hsm) provides open access to all the land cover/change and validation data presented in this article as well as technical reports and on the fly statistics.

7. Conclusions and Outlook

The C-HSM service component is part of Copernicus Global Land, which produces near real time biophysical variables at medium scale, globally. In contrast, the C-HSM activity is an on-demand component that addresses specific user requests in the field of sustainable management of natural resources. The products presented here provide the first set of standardized land cover and land cover change datasets for 12 KLCs with their corresponding validation datasets in Sub-Saharan Africa. The geographic distribution covers the tropical and subtropical regions of West, Central and South-Eastern Africa. The next release will also include countries in the Caribbean and Pacific areas of the ACP region and some areas beyond these regions may be mapped depending on user demands. The most recent land cover change will be reassessed for selected already-mapped KLC's in order to generate longer-term time series land cover dynamics information. While this is not done systematically, but on specific customer requests, the C-HSM service encourages stakeholder cooperation and provides capacity building workshops around the globe. In person training events provide an opportunity for new and existing users to learn how to use and interpret data, operate the web information system, and easily assess recent land cover change data using Sentinel 2 image mosaics. Here, we provide very high-quality products, which can be used directly as base maps and for policy decisions, as well as for comparison and/or evaluation of other land cover products or the implementation of validation datasets for training/validation purposes.

Finally, the service has a high degree of confidence that the data presented here (and the next phase) are of highest quality, reaching regularly above 90% overall accuracy. This is guaranteed by a rigorous and independent production-validation mechanism and feedback loop, which does not stop until the required overall, and per-class accuracy levels are reached.

Following the general European Commission's Copernicus Programme open access policy, the data is distributed free to any user through a dedicated website (https://land.copernicus.eu/global/hsm). This interactive online information system allows access to browse, analyse and download the data, including the accuracy assessment information.

Appendix Information

Appendix A contains the thematic class accuracies for each KLC, both land cover and land cover maps.

CLASS_A - Corresponding class (see Table 2 'Dichotomous map code') - OR

CLASS_B - Corresponding class (see Table 2 'Modular map code')

PA - Producer's accuracy

UA - User's accuracy

NoRP - number of reference points

Appendix A.

Thematic class accuracies per KLC*

*Accuracy parameters are in percent, classes with less than 15 samples were not included in the overall accuracy calculation.

CAF01							
2000				2016			
CLASS_B	PA	UA	NoRP	CLASS_B	PA	UA	NoRP
3	96.3	93.9	903	11	98.1	96.4	64
4	90.4	96.6	1061	31	94.7	89.3	283
6	100	90	46	32	86.5	90.4	61
7	95.8	93.5	206	33	77	93.5	7
11	98.2	96.4	63	34	74	43.3	12
13	100	93.4	57	55	92.4	100	62
14	95.4	91.2	159	56	99.5	96.7	91
77	97.5	96.5	654	59	89.4	82.4	45
78	91.8	84.9	429	60	90.3	90.7	401
165	96.7	89.5	106	77	97.7	96.2	584
166	69.3	83.6	15	78	90.6	85.3	414
184	99.7	94.1	100	112	81.6	92.8	458
185	89.3	89.6	44	116	92	87.7	270
				148	87	92.8	225
				152	84.4	99.5	25
				160	100	89.8	46
				165	96.6	89.3	108
				166	73.9	84.7	15
				171	94.3	94.1	103
				175	69.6	61.1	4
				178	99.9	92	97
				184	99.7	93.9	172
				185	97	89.1	83
				187	95.3	96.7	61
				190	95.7	90.9	97

191	100	95	61

CAF02							
2001				2015			
CLASS_B	PA	UA	NoRP	CLASS_B	PA	UA	NoRP
3	95.4	95.7	1523	11	99.9	98.8	130
4	86.5	91.7	1054	31	64.9	88.3	150
6	0	0	1	32	89.5	91	287
7	87.4	84.3	362	33	0	0	1
11	88.9	92.9	94	34	88.1	95.5	123
14	99.6	99.7	370	55	87.5	60.3	9
77	93.2	87	686	56	92.9	88.3	558
78	65.3	67.7	160	59	69.8	93.6	27
165	50.5	38.3	8	60	89.5	93.9	569
166	86.9	85.3	16	77	96.5	91.6	544
184	87	89.8	122	78	61.2	74.7	153
185	97.7	81.1	39	112	82.4	76.8	237
192	100	100	30	116	90.9	85	269
				148	86.1	92	322
				152	94	99.3	3
				160	0	0	1
				165	77.8	37.6	7
				166	56.2	85.1	16
				171	82.3	84.8	176
				175	63.8	56.9	15
				178	84.7	72.3	214
				182	100	69.2	1
				184	88.9	98.1	213
				185	89.6	58	44
				190	88.3	99.2	80
				191	100	99.6	286
				192	100	100	30

355

CAF06							
2003				2015			
CLASS_B	PA	UA	NoRP	CLASS_B	PA	UA	NoRP
3	82.6	91.5	236	55	100	100	47
4	88.9	93.3	1882	60	80.5	89.1	199
7	98.3	76.1	422	77	83.4	92.2	656
14	99.4	90.5	103	78	85.8	77.2	738
77	83.5	92.1	680	112	85.7	90.7	1427
78	85.8	77.2	749	116	83.2	84.3	280
184	91.9	89.9	73	148	90.5	91.5	127
				171	96.4	64.3	113
				175	96.5	70	123
				178	87.8	88.4	173
				184	93.4	91	128
				190	99.4	90	71
				191	100	99.8	32

CAF07							
2000				2016			
CLASS_A	PA	UA	NoRP	CLASS_A	PA	UA	NoRP
3	96	89.4	120	3	99.7	96.5	127
4	99.4	99.9	847	4	99.5	100	836
7	100	97.6	255	7	100	97.6	255
10	100	89.7	61	10	100	94.2	65
14	100	99.2	81	14	100	99.2	81

CAF11							
2000				2016			
CLASS_B	PA	UA	NoRP	CLASS_B	PA	UA	NoRP
3	98.7	92.8	320	11	100	100	30
4	99.3	93.8	1125	32	100	100	26
6	100	14.4	1	34	0	0	0

7	96.9	99.2	618	56	69.9	100	2
11	100	96.7	29	59	92.4	99.1	75
14	98.7	99.9	278	60	97.3	97.1	334
77	94.5	95.6	539	77	94.6	95.2	488
78	92.6	97.7	652	78	92.4	97.1	584
165	79.4	96.3	77	112	96.8	86.9	405
166	98.7	99.2	48	116	97.7	94.3	284
184	100	95.8	83	148	98.5	97.1	321
185	100	95.4	15	152	0	0	0
				160	100	100	3
				165	79.1	96.2	76
				166	96.9	99.2	47
				171	75	92.7	77
				175	56.8	98.6	74
				178	97.9	98	411
				182	95	95	20
				184	100	98.9	161
				185	100	100	75
				190	87.9	98.2	89
				191	99.8	100	203

CAF15							
2000				2016			
CLASS_B	PA	UA	NoRP	CLASS_B	PA	UA	NoRP
3	100	82.8	80	77	99.7	99.5	1936
4	98.3	95.8	546	78	94.1	91.9	257
7	78.5	94.2	108	112	93.1	92.7	379
14	98.2	96.9	97	116	0	0	3
77	99.7	99.5	2048	148	98.9	97.2	306
78	91.9	92.4	303	152	100	86.4	57
165	94.1	98.7	348	165	94.1	98.8	300
166	100	81.4	72	166	100	81.2	63

184	98.3	95.8	85	171	74.2	88.7	41
				175	0	0	1
				178	83.5	95.8	69
				184	100	99.7	178
				190	98.2	96.9	97

CAF16							
2000				2016			
CLASS_A	PA	UA	NoRP	CLASS_A	PA	UA	NoRP
3	96.8	72.5	93	3	88.3	84.6	142
4	99.5	99.7	848	4	99.3	99.5	761
7	86.4	82.6	94	7	85.7	82.6	94
10	96.2	98.1	55	10	97.3	98.7	94
13	100	98.7	75	13	100	94.7	75
14	96.1	94.9	73	14	96.1	94.9	73

360

CAF99							
2000				2016			
CLASS_B	PA	UA	NoRP	CLASS_B	PA	UA	NoRP
3	91.6	98.9	431	31	91.6	99.8	267
4	92.4	92.1	417	32	94.5	100	69
7	100	97.8	231	56	100	99.5	76
14	100	100	175	59	100	9.5	4
77	99	99.2	905	60	91.9	96.5	125
78	93.6	85.1	210	77	99.6	99.2	732
165	97.8	97.9	246	78	79.1	91.5	156
166	100	88.7	40	112	96.1	95.9	341
184	99.4	88.3	72	148	98.7	96.9	168
				165	97.8	97.5	240
				166	100	89.2	42
				171	100	100	102
				175	0	0	3

178	100	91.6	77
184	100	95.9	150
185	100	100	2
190	100	100	113
191	100	100	60

SAF02							
2002				2016			
CLASS_B	PA	UA	NoRP	CLASS_B	PA	UA	NoRP
3	93.9	94.9	705	11	98.3	100	3
4	96.1	96	1425	31	100	86.1	66
6	100	67	1	33	93.8	88.1	104
7	94.7	91.3	170	34	98.1	76.8	140
11	100	100	2	55	84.1	40.3	30
13	91.9	98.3	76	56	55	100	3
14	91.5	92.7	146	59	96.6	95	185
77	84.7	75.8	204	60	91.7	92.7	165
78	81.2	85.1	392	77	85	74.3	154
165	11.4	84.1	7	78	79	87.2	400
166	90.8	98.6	17	112	96.8	94.7	880
184	92.7	92.6	142	116	90.9	96.2	284
185	100	94.7	67	148	77.6	94.2	122
				152	85.1	87.6	108
				160	100	100	3
				165	0	0	4
				166	91.6	100	13
				171	98.5	90.8	100
				175	78.9	78	35
				178	92.6	93.9	42
				182	100	50	2
				184	94.8	97.3	211
				185	100	95.1	93

187	95.9	98.4	83
190	96.6	99.2	100
191	83.7	87.3	24

SAF14/15							
2000				2015			
CLASS_A	PA	UA	NoRP	CLASS_A	PA	UA	NoRP
3	91	94.8	215	3	95.9	95.2	301
4	98.7	99.2	845	4	98.6	99.2	756
7	93.4	84.2	73	7	93.5	88.6	74
10	96	81.6	67	10	96.8	84.6	77
11	100	100	42	11	100	100	42
14	85.1	87.4	85	14	85.2	87.4	85

WAF05							
2000				2015			
CLASS_A	PA	UA	NoRP	CLASS_A	PA	UA	NoRP
3	77.2	97.6	217	3	83.2	99.3	310
4	99.5	97.4	735	4	99.6	96.1	583
6	0	0	0	6	0	0	0
7	98.5	77.9	26	7	81.6	77.9	26
10	95.2	93.2	77	10	100	98.1	138
11	100	100	57	11	100	100	57
13	100	96	72	13	100	93.3	70
14	100	100	74	14	100	100	74

WAF10							
2001				2016			
CLASS_B	PA	UA	NoRP	CLASS_B	PA	UA	NoRP
3	96	98.6	1518	11	100	100	32
4	94.5	100	151	31	94.2	99.3	275
6	66.9	100	44	32	87.3	100	3

7	99.2	93.8	79	33	100	50	1
11	100	100	32	34	100	92.7	22
13	100	100	109	55	0	0	13
14	99.3	100	94	56	99.5	97.8	1153
77	99.5	98.8	2017	59	0	0	2
78	93.3	91.5	215	60	95	98.3	327
165	100	96.8	43	77	99.5	99.6	1695
166	0	0	0	78	93.4	90.8	189
184	99.3	98.9	83	112	98.8	95.7	32
185	0	0	0	116	100	100	1
				148	98.6	99.9	100
				152	0	0	1
				160	68.1	100	50
				165	88.9	96.8	44
				166	0	0	1
				171	100	96.9	59
				178	99	86.7	20
				184	93.5	100	159
				185	100	42.1	2
				187	100	100	109
				190	98.9	100	95
				191	0	0	0

Supplement. The supplement related to this article is available online at: https://doi.org/10.5194/essd-2020-77-supplement (please see STable 1).

STable 1 contains references to the data which have been used to create the land cover/change maps for each KLC.

Sensor:

L8 - Landsat 8 imagery

L7 - Landsat 7 imagery

L5 - Landsat 5 imagery

Date (acquisition of the imagery): YYYYMMDD - year - month - day format

Path/Row of the Imagery used: Worldwide Reference System for Landsat data (i.e. scene location on the globe)

Author contribution: ZSZ and ABB designed the work. CM and GJ implemented the workflows. ZSZ and ABB wrote the paper. ZSZ, ABB, AL and GJ revised the paper.

Acknowledgements. The development of the thematic maps have been made possible thanks to the effort of ITHACA (Information Technology for Humanitarian Assistance, Cooperation and Action) and Telespazio - a LEONARDO And THALES company; and their quality evaluations by IGNFI (France), Joanneum Research (Austria), EOXPLORE (Germany), GISBOX (Romania), Space4environment (Luxembourg), ONFI (France) and LuxSpace (Luxembourg). The authors also thank Mr. A. McKinnon (EC/JRC) for proofreading the paper.

Competing interests. The authors declare that they have no conflict of interest.

Disclaimer. All features and data are provided "as is" with no warranties of any kind.

Review statement. This paper was edited by Dr. David Carlson and reviewed by 3 anonymous referees.

References

Brink, A., Eva, H. and Bodart, C.: Is Africa Losing Its Natural Vegetation?: Monitoring Trajectories of Land-Cover Change Using Landsat Imagery, in Remote Sensing of Land Use and Land Cover, vol. 20120991, pp. 369–376, CRC Press., 2012.

Brink, A. B. and Eva, H. D.: Monitoring 25 years of land cover change dynamics in Africa: A sample based remote sensing approach, Appl. Geogr., 29(4), 501–512, doi:10/fqg9cc, 2009.

Di Gregorio, A.: Land cover classification system: classification concepts and user manual: LCCS, Software version 2., Food and Agriculture Organization of the United Nations, Rome., 2005.

Di Minin, E., Slotow, R., Hunter, L. T. B., Montesino Pouzols, F., Toivonen, T., Verburg, P. H., Leader-Williams, N., Petracca, L. and Moilanen, A.: Global priorities for national carnivore conservation under land use change, Sci. Rep., 6(1), doi:10/f8gmf9, 2016.

Dinerstein, E., Olson, D., Joshi, A., Vynne, C., Burgess, N. D., Wikramanayake, E., Hahn, N., Palminteri, S., Hedao, P., Noss, R., Hansen, M., Locke, H., Ellis, E. C., Jones, B., Barber, C. V., Hayes, R., Kormos, C., Martin, V., Crist, E., Sechrest, W., Price, L., Baillie, J. E. M., Weeden, D., Suckling, K., Davis, C., Sizer, N., Moore, R., Thau, D., Birch, T., Potapov, P., Turubanova, S., Tyukavina, A., de Souza, N., Pintea, L., Brito, J. C., Llewellyn, O. A., Miller, A. G., Patzelt, A., Ghazanfar, S. A., Timberlake, J., Klöser, H., Shennan-Farpón, Y., Kindt, R., Lillesø, J.-P. B., van Breugel, P., Graudal, L., Voge, M., Al-Shammari, K. F. and Saleem, M.: An Ecoregion-Based Approach to Protecting Half the Terrestrial Realm, BioScience, 67(6), 534–545, doi:10/gbh29s, 2017.

European Commission: Science for the AU-EU Partnership building knowledge for sustainable development., Joint Research Centre., 2018.

Fritz, S., See, L., Perger, C., McCallum, I., Schill, C., Schepaschenko, D., Duerauer, M., Karner, M., Dresel, C., Laso-Bayas, J.-C., Lesiv, M., Moorthy, I., Salk, C. F., Danylo, O., Sturn, T., Albrecht, F., You, L., Kraxner, F. and Obersteiner, M.: A global dataset of crowdsourced land cover and land use reference data, Sci. Data, 4(1), 1–8, doi:10.1038/sdata.2017.75, 2017.

Gallaun, H., Steinegger, M., Wack, R., Schardt, M., Kornberger, B. and Schmitt, U.: Remote Sensing Based Two-Stage Sampling for Accuracy Assessment and Area Estimation of Land Cover Changes, Remote Sens., 7(9), 11992–12008, doi:10.3390/rs70911992, 2015.

Geist, H. J. and Lambin, E. F.: Proximate Causes and Underlying Driving Forces of Tropical Deforestation, BioScience, 52(2), 143, doi:10.1641/0006-3568(2002)052[0143:PCAUDF]2.0.CO;2, 2002.

Hagolle, O., Huc, M., Villa Pascual, D. and Dedieu, G.: A Multi-Temporal and Multi-Spectral Method to Estimate Aerosol Optical Thickness over Land, for the Atmospheric Correction of FormoSat-2, LandSat, VENμS and Sentinel-2 Images, Remote Sens., 7(3), 2668–2691, doi:10/ggfq48, 2015.

Kebede, E., Kagochi, J. and Jolly, C. M.: Energy consumption and economic development in Sub-Sahara Africa, Energy Econ., 32(3), 532–537, doi:10.1016/j.eneco.2010.02.003, 2010.

MacKinnon, J., Aveling, C., Olivier, R., Murray, M., Paolini, C., European Commission and Directorate-General for International Cooperation and Development: Larger than elephants: inputs for an EU strategic approach to wildlife conservation in Africa : synthesis. [online] Available from: http://dx.publications.europa.eu/10.2841/909032 (Accessed 24 April 2018), 2015.

Marshall, M., Norton-Griffiths, M., Herr, H., Lamprey, R., Sheffield, J., Vagen, T. and Okotto-Okotto, J.: Continuous and consistent land use/cover change estimates using socio-ecological data, Earth Syst. Dyn., 8(1), 55–73, doi:https://doi.org/10.5194/esd-8-55-2017, 2017.

Masek, J. G., Vermote, E. F., Saleous, N. E., Wolfe, R., Hall, F. G., Huemmrich, K. F., Gao, F., Kutler, J. and Lim, T.-K.: A Landsat Surface Reflectance Dataset for North America, 1990–2000, IEEE Geosci. Remote Sens. Lett., 3(1), 68–72, doi:10/b2w5mc, 2006.

van der Meer, E.: Carnivore conservation under land use change: the status of Zimbabwe's cheetah population after land reform, Biodivers. Conserv., 27(3), 647–663, doi:10/gc3dhq, 2018.

Mora, B., Tsendbazar, N.-E., Herold, M. and Arino, O.: Global Land Cover Mapping: Current Status and Future Trends, in Land Use and Land Cover Mapping in Europe, vol. 18, edited by I. Manakos and M. Braun, pp. 11–30, Springer Netherlands, Dordrecht., 2014.

Nissan, H., Goddard, L., de Perez, E. C., Furlow, J., Baethgen, W., Thomson, M. C. and Mason, S. J.: On the use and misuse of climate change projections in international development, Wiley Interdiscip. Rev. Clim. Change, 10(3), e579, doi:10.1002/wcc.579, 2019.

Saah, D., Tenneson, K., Poortinga, A., Nguyen, Q., Chishtie, F., Aung, K. S., Markert, K. N., Clinton, N., Anderson, E. R., Cutter, P., Goldstein, J., Housman, I. W., Bhandari, B., Potapov, P. V., Matin, M., Uddin, K., Pham, H. N., Khanal, N., Maharjan, S., Ellenberg, W. L., Bajracharya, B., Bhargava, R., Maus, P., Patterson, M., Flores-Anderson, A. I., Silverman, J.,

Sovann, C., Do, P. M., Nguyen, G. V., Bounthabandit, S., Aryal, R. R., Myat, S. M., Sato, K., Lindquist, E., Kono, M., Broadhead, J., Towashiraporn, P. and Ganz, D.: Primitives as building blocks for constructing land cover maps, Int. J. Appl. Earth Obs. Geoinformation, 85, 101979, doi:10.1016/j.jag.2019.101979, 2020.

Stehman, S. V.: Impact of sample size allocation when using stratified random sampling to estimate accuracy and area of land-cover change, Remote Sens. Lett., 3(2), 111–120, doi:10.1080/01431161.2010.541950, 2012.

Strobl, P., Baumann, P., Lewis, A., Szantoi, Z., Killough, B., Purss, M. B. J., Craglia, M., Nativi, S., Held, A. and Dhu, T.: The six faces of the data cube, in Proc. of the 2017 conference on Big Data from Space (BiDS'17), Luxembourg: Publications Office of the European Union, 2017, Toulouse, France., 2017.

Sylla, M. B., Pal, J. S., Wang, G. L. and Lawrence, P. J.: Impact of land cover characterization on regional climate modeling over West Africa, Clim. Dyn., 46(1–2), 637–650, doi:10.1007/s00382-015-2603-4, 2016.

Szantoi, Z., Escobedo, F., Abd-Elrahman, A., Smith, S. and Pearlstine, L.: Analyzing fine-scale wetland composition using high resolution imagery and texture features, Int. J. Appl. Earth Obs. Geoinformation, 23, 204–212, doi:10/gdnfvd, 2013.

Szantoi, Z., Brink, A., Buchanan, G., Bastin, L., Lupi, A., Simonetti, D., Mayaux, P., Peedell, S. and Davy, J.: A simple remote sensing based information system for monitoring sites of conservation importance, Remote Sens. Ecol. Conserv., 2(1), 16–24, doi:10.1002/rse2.14, 2016.

Szantoi, Z., Brink, A., Lupi, A., Mannone, C., and Jaffrain, G.: Land cover and change thematic and validation datasets for Sub-Saharan Africa. PANGAEA, https://doi.pangaea.de/10.1594/PANGAEA.914261

Szantoi, Z., Geller, G. N, Tsendbazar, N-E., See, L., Griffiths, P., Fritz, S., Gong, P., Herold, M., Mora, B., Obregon, A.: Addressing the Need for Improved Land Cover Map Products for Policy Support, Environ. Sci. & Pol., 112, 28-35, doi: 10.1016/j.envsci.2020.04.005

Tolessa, T., Senbeta, F. and Kidane, M.: The impact of land use/land cover change on ecosystem services in the central highlands of Ethiopia, Ecosyst. Serv., 23, 47–54, doi:10.1016/j.ecoser.2016.11.010, 2017.

Tsendbazar, N.-E., Herold, M., de Bruin, S., Lesiv, M., Fritz, S., Van De Kerchove, R., Buchhorn, M., Duerauer, M., Szantoi, Z. and Pekel, J.-F.: Developing and applying a multi-purpose land cover validation dataset for Africa, Remote Sens. Environ., 219, 298–309, doi:10/gfqggv, 2018.

Vondou, D. A. and Haensler, A.: Evaluation of simulations with the regional climate model REMO over Central Africa and the effect of increased spatial resolution: EVALUATION OF REMO RESOLUTION OVER CENTRAL AFRICA, Int. J. Climatol., 37, 741–760, doi:10.1002/joc.5035, 2017.

Zhu, Z., Wang, S. and Woodcock, C. E.: Improvement and expansion of the Fmask algorithm: cloud, cloud shadow, and snow detection for Landsats 4–7, 8, and Sentinel 2 images, Remote Sens. Environ., 159, 269–277, doi:10/f67rhz, 2015.